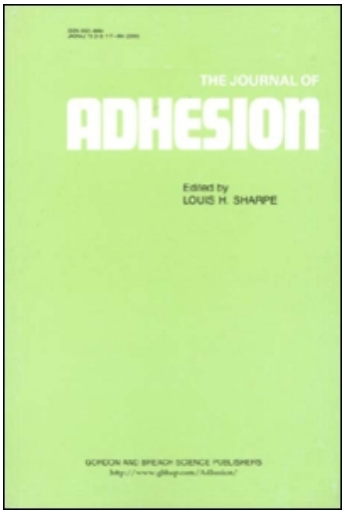

The Journal of Adhesion
Publication details, including instructions for authors and subscription information:
http://www.informaworld.com/smpp/title~content=t713453635

CRITICAL SELF-ASSEMBLY CONCENTRATION OF AN IONIC-COMPLEMENTARY PEPTIDE EAK16-I

Yooseong Hong[a]; Lue Shunn Lau[a]; Raymond L. Legge[a]; P. Chen[a]
[a] Department of Chemical Engineering, University of Waterloo, Waterloo, Ontario, Canada

Online publication date: 10 August 2010

To cite this Article Hong, Yooseong , Lau, Lue Shunn , Legge, Raymond L. and Chen, P.(2004) 'CRITICAL SELF-ASSEMBLY CONCENTRATION OF AN IONIC-COMPLEMENTARY PEPTIDE EAK16-I', The Journal of Adhesion, 80: 10, 913 — 931
To link to this Article: DOI: 10.1080/00218460490508616
URL: http://dx.doi.org/10.1080/00218460490508616

The Journal of Adhesion, 80: 913–931, 2004

ISSN: 0021-8464 print/1545-5823 online
DOI: 10.1080/00218460490508616

Taylor & Francis
Taylor & Francis Group

CRITICAL SELF-ASSEMBLY CONCENTRATION OF AN IONIC-COMPLEMENTARY PEPTIDE EAK16-I

Yooseong Hong
Lue Shunn Lau
Raymond L. Legge
P. Chen
Department of Chemical Engineering, University of Waterloo, Waterloo, Ontario, Canada

Understanding the process of self-assembly of peptides has been important in various biomedical engineering applications. This work focuses on the effect of peptide concentration on the molecular self-assembly of an ionic-complementary peptide, EAK16-I (AEAKAEAKAEAKAEAK), in aqueous solution. The surface tension and self-assembled nanostructures were determined for a wide range of peptide concentrations using axisymmetric drop shape analysis-profile (ADSA–P) and atomic force microscopy (AFM), respectively. Surface tension measurements revealed a critical self-assembly concentration of 0.3 mg peptide/ml water, below which the surface tension decreased rapidly with increasing peptide concentration, and above which the surface tension remained at a constant, plateau value. There were two structural transitions observed with increasing peptide concentration: the first was from globular nanostructures to fibrils, and the second from the fibrils to relatively thick fibers. The second structural transition occurred at the critical self-assembly concentration as determined by the surface tension measurements. The nanostructural behavior of EAK16-I was compared with that of EAK16-II, which has the same amino acid composition but a different charge distribution. Salt effects were also examined by adding NaCl to the peptide solution. The salt addition facilitated the formation of peptide fibrils at low peptide concentrations but increased the critical self-assembly concentration, which occurred at 0.8 mg peptide/ml water in the presence of 20 mM NaCl. The structural transitions

Received 11 December 2003; in final form 7 June 2004.

We thank Professor Jean Duhamel, Shane Fung and Bobby Dhadwar for helpful discussions. This research was financially supported by the National Sciences and Engineering Research Council of Canada (NSERC), Canadian Foundation for Innovation (CFI), and the Premier's Research Excellence Award (PREA).

One of a collection of papers honoring A. W. Neumann, the recipient in February 2004 of *The Adhesion Society Award for Excellence in Adhesion Science, Sponsored by 3M*.

Address correspondence to P. Chen, Department of Chemical Engineering, University of Waterloo, 200 University Avenue West, Waterloo, Ontario, Canada N2L 3G1. E-mail: p4chen@cape.uwaterloo.ca

involved in the self-assembly of EAK16-I resemble those from protofibrils to fibrils observed with numerous naturally occurring peptides. An understanding of this structural transition may have relevance in the analysis and treatment of peptide/protein conformational diseases and have application in the production of self-assembled protein nanostructures.

Keywords: Self-assembly; Peptides; Critical self-assembly concentration; Surface tension; Nanostructural transition; Atomic force microscopy; Axisymmetric drop shape analysis–profile

INTRODUCTION

The ability of nature to direct the assembly of biological components into organized and sophisticated supramolecular structures has motivated research into the fundamentals of biomolecular self-assembly. Self-assembling peptides, which are relatively easy to design and synthesize, have been found to have versatile biomedical applications, including scaffolding for tissue engineering [1–3], controlled drug delivery [4, 5] and surface engineering [6–11]. More recent applications include the use of self-assembled peptide monolayers for biosensors [8, 9] and molecular electronics [10, 11]. However, the application of peptide self-assembly has been hampered by lack of control methods, largely due to a poor understanding of the molecular mechanisms governing self-assembling.

To understand the self-assembly mechanisms of a given peptide, it is important to understand the factors that govern the peptide's self-assembling behavior. The physicochemical factors that influence the self-assembly process may include: (1) amino acid sequence, which determines the primary structure of a peptide; (2) concentration of the peptide; (3) molecular size, such as the length or molecular weight of the peptide; and (4) solution conditions (*e.g.*, pH and ionic strength, temperature, solvent composition, and substrate). Of these factors, amino acid sequence, pH [12], and peptide concentration [13] have been investigated for the ionic-complementary peptides, EAK16-II (AEAEAKAKAEAEAKAK) and EAK16-IV (AEAEAEAEAKAKAKAK). Recently, Fung *et al*. studied the effect of peptide concentration on self-assembly behavior using several independent techniques, such as surface tension measurement, atomic force microscopy (AFM), and light scattering [13]. The results indicated that there is a critical aggregation concentration, or "critical self-assembly concentration," for the self-assembly of this series of peptides.

The critical self-assembly concentration can be understood by analogy to the critical micelle concentration (CMC) of surfactants. This well-known phenomenon is related to the chemical and structural properties

of surfactant molecules. A typical surfactant molecule has a hydrophilic head and hydrophobic tail, which makes the molecule amphiphilic. When enough surfactant molecules exist in a polar solvent, they will form a micelle to minimize entropically unfavorable interactions of hydrophobic tails with the polar solvent molecules. A peptide can also be amphiphilic because of the presence of hydrophobic and hydrophilic amino acids and thus is expected to show similar concentration-dependent self-assembly, leading to the formation of nanostructures.

For the ionic-complementary peptides of interest, Hong *et al*. [12] recently found that the self-assembly process is dependent on the charge distribution along the peptide backbone. Further work by Jun *et al*. [14] confirmed that the charge distribution is the determining factor in single molecule conformation, which in turn dictates the resulting nanostructure formation for a series of ionic-complementary peptides EAK16-I, II and IV. Therefore, it is critical to understand how the charge distribution affects the critical self-assembly concentration.

The peptide used in this study was EAK16-I (AEAKAEAKAEAKAEAK), one of the self-assembling, ionic-complementary peptides [3, 7, 15–17]. This peptide is simple yet possesses all the major physicochemical interactions for self assembly, including hydrogen bonding between peptide backbones, hydrophobic interactions between hydrophobic amino acid residues (Ala), and electrostatic interactions between amino acids with charged side groups (Glu and Lys). It is known that the presence of alternating hydrophobic and hydrophilic amino acids (see Figure 1) favors the formation of β-sheets [18]. The presence of alternating opposite charges on the hydrophilic face gives this peptide ionic self-complementarity [16]. The purpose of this study was to examine: (1) how peptide concentration affects the self-assembly of this ionic-complementary peptide in water; (2) how the self-assembled nanostructures correlate with the surface

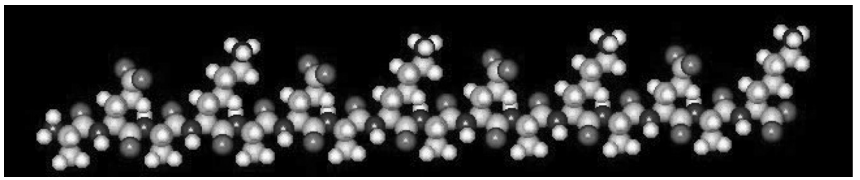

FIGURE 1 Three-dimensional molecular structure of EAK16-I (AEAKAEAKAEAKAEAK). Two distinct faces can be present because the hydrophobic (Ala) and hydrophilic amino acids (Glu, and Lys) alternate. In addition, negative-(Glu) and positive-(Lys) charged amino acids alternate along the hydrophilic face. Carbon is in blue, hydrogen in white, nitrogen in purple, and oxygen in red (See Color Plate I).

properties of the peptide solution; and (3) how the self-assembling behavior of EAK16-I compares with that of a similar ionic-complementary peptide, EAK16-II. The effect of an ionic salt on this process was also studied, as various salts have been known to affect the solubility, denaturation, and association and dissociation of macromolecules [19–22]. For example, ionic salts are known to affect the formation of micelles by surfactants, often decreasing the CMC by charge screening of the hydrophilic heads of the surfactants [23–25]. The presence of ionic salts has also been shown to affect biomolecular self-assembly, such as the effect of multivalent salts on DNA condensation [26, 27].

MATERIALS AND METHODS

Materials

EAK16-I ($C_{70}H_{121}N_{21}O_{25}$, molecular weight 1657) was purchased from Invitrogen (Huntsville, AL, USA), and used without further purification. The N-terminus and C-terminus of the peptide were protected by acetyl and amino groups, respectively. Peptide solutions were prepared at concentrations from 0.01 to 4.0 mg/ml of pure water (18 ΩM; Millipore Milli-Q system). In the case of experiments examining the effect of NaCl, peptides' were added to a 20 mM NaCl solution at the various final peptide concentrations from 0.01 to 4.0 mg/ml. Salt effects over a range of 0.1 to 20 mM were also examined at a peptide concentration of 0.01 mg/ml. All peptide solutions were stored at 4°C before use.

Axisymmetric Drop Shape Analysis–Profile (ADSA–P)

Axisymmetric drop shape analysis–profile (ADSA–P) was used to measure the surface tension of EAK16-I solutions at an air–water interface. A pendant drop of the peptide solution was formed at the tip of a vertical Teflon® capillary, which was connected to a motor-driven microsyringe, producing an axisymmetric drop boundary. This was done in a temperature-controlled environmental chamber saturated with water vapor. The entire system was isolated on a vibration-free table. The image of the pendant drop was acquired using an optical microscope and a CCD camera and digitally recorded for 1 h after the pendant drop was formed. Software was used to digitize the image and generate a profile of the pendant drop. A theoretical curve, governed by the Laplace equation of capillarity, was then fitted to the profile, generating the surface tension value as a fitting parameter [13, 28]. The typical standard deviations of all measurements were less than 0.2 mJ/m^2.

Atomic Force Microscopy (AFM)

Atomic force microscopy (AFM) was used to observe the nanostructure of the peptide self-assemblies. Approximately 10 μl of the peptide solution was placed on the surface of a freshly cleaved mica sheet that was glued to a steel AFM sample plate. The sample was incubated for 10 min under the ambient conditions before being washed with approximately 100 μl of pure water (18 MΩ; Millipore Milli-Q system) to remove free peptides. After air drying for 3 h, AFM imaging was performed at room temperature using the tapping mode on a PicoScan™ AFM (Molecular Imaging, Phoenix, AZ, USA). All images were acquired using a 225 μm silicon single-crystal cantilever (type NCL, Molecular Imaging, Phoenix, AZ, USA) with a typical tip radius of 10 nm and frequency of 165 kHz. A scanner with maximum scan sizes of $6 \times 6\,\mu m^2$ was used (calibrated with a standard calibration grid consisting of $1 \times 1\,\mu m^2$ squares). All AFM images had a resolution of 512×512 pixels. AFM imaging was also performed on a hydrophobic substrate, graphite, and showed no significant differences.

RESULTS AND DISCUSSION

Critical Self-assembly Concentration by Surface Tension Measurements

The effect of peptide concentration on surface tension is given in Figure 2. At low peptide concentrations (0.01 mg/ml), the surface tension does not change significantly with time. At high concentrations, greater than 0.3 mg/ml, the surface tension rapidly decreases with time (between 0 to 200 s) and then slowly reaches a constant, lower equilibrium value. The surface tension profile of the EAK16-I solutions at low peptide concentrations is characterized by an initial induction time, which is frequently found in biomolecular systems [13].

Because the time-dependent surface tension profiles do not reach an absolute steady state after 1 h, estimation of the equilibrium surface tension is required. Two methods were used in this study to estimate the equilibrium surface tension value from the time-dependent surface tension profile [28]. The first method was the "end points" method; the equilibrium surface tension is calculated by averaging a certain number of data points at the end of the measurement, and 15 data points were averaged in the present study. The second method is the "extrapolation" method; at the end of 1 h, a portion of the surface tension curve that showed linearity with respect to $1/t^{0.5}$ was fitted to a straight line, and the y intercept was used as an estimate of the equilibrium surface tension.

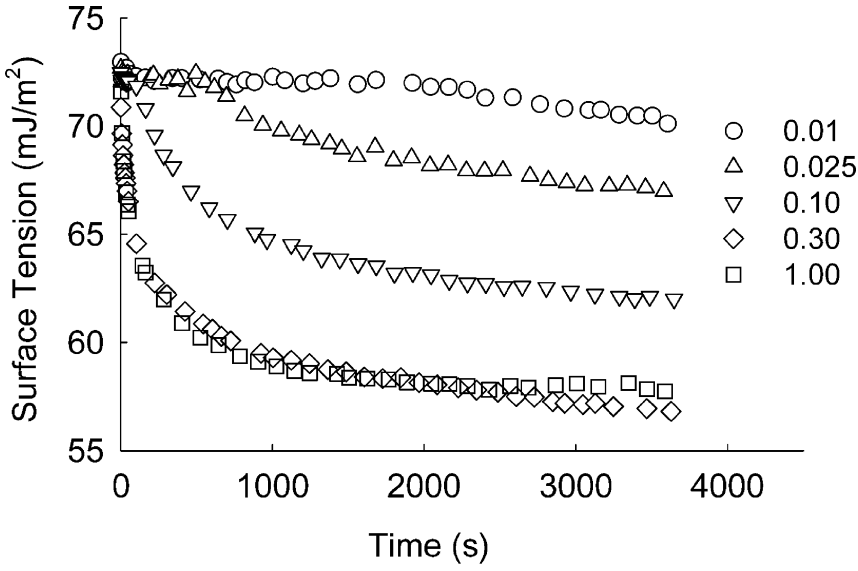

FIGURE 2 Dynamic surface tension profile for selected concentrations; 0.01 (◯), 0.025 (△), 0.10 (▽), 0.3 (◇), and 1.0 mg/ml (□), of EAK16-I obtained with ADSA-P over a 1 h time period. At low peptide concentrations (0.01 mg/ml) the surface tension is close to that of pure water (72.8 mJ/m^2).

Figure 3a shows the estimated equilibrium surface tension as a function of the peptide concentration using the "end points" method. The equilibrium surface tension plot shows that there is a dependence of surface tension on peptide concentration. At the lowest EAK-16-I concentration, 0.01 mg/ml, the surface tension (*ca.* 71 mJ/m^2) is similar to that of pure water (*ca.* 72 mJ/m^2). The surface tension decreases with increasing peptide concentration until the peptide concentration reaches 0.3 mg/ml. Above this concentration, the equilibrium surface tension essentially remains constant. Figure 3b is a plot of induction time *versus* peptide concentration. Induction time was determined as the time when the surface tension decreased by 5% from the initial value. The induction time decreases as peptide concentration increases, until the peptide concentration reaches 0.3 mg/ml, above which there is essentially no induction time. This change in induction time reflects a critical change in surface properties of the peptide solution. The peptide concentration, at which the induction time showed a critical change, is consistent with the concentration at which the equilibrium surface tension showed a critical change.

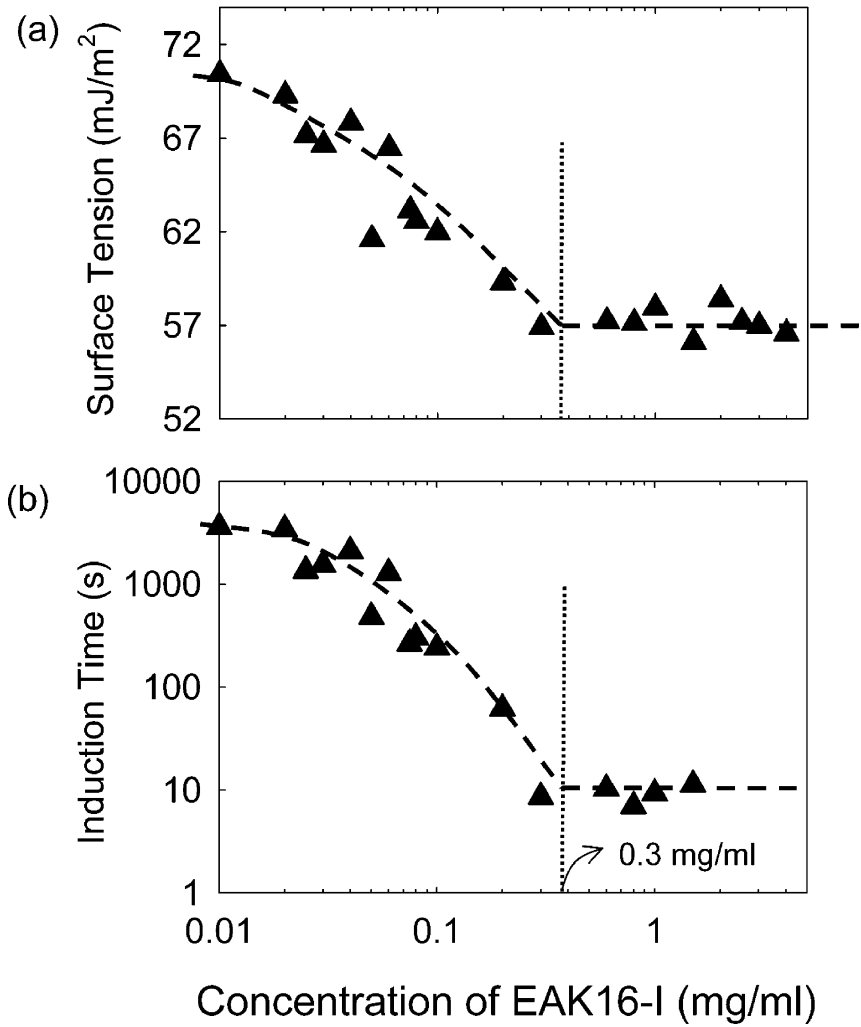

FIGURE 3 (a) Estimated equilibrium surface tension and (b) the induction time as a function of EAK16-I concentration. The equilibrium surface tension was determined by the "end points" method (see text), and the induction time was determined as the time when the surface tension decreased by 5% from the initial value.

An induction time is commonly observed in dynamic surface tension measurements for surface-active biomolecules [13]. It is proposed that the induction time represents the time required for the surface monolayer to attain a certain minimum coverage, above which the surface

tension decreases [29]. It is also proposed that proteins do not change the surface tension until they change conformation and rearrange at the surface [30]. These propositions seem to be applicable to the present results. When the bulk concentration of EAK16-I increases, more EAK16-I molecules adsorb onto the air–water interface, resulting in a decrease in the induction time, as is shown in Figure 3b. EAK16-I molecules that adsorbed onto the interface may rearrange to form self-assembled β-sheet monolayers, providing effective surface coverage, eventually significantly decreasing the surface tension. When the concentration is high enough, above the critical concentration, EAK16-I molecules can form self-assembled structures in the bulk and then adsorb onto the interface. The adsorption of self-assembled structures could be more effective than those of a single molecule in reducing surface tension; therefore, a nearly zero induction time was observed.

Comparison of the Critical Self-assembly Concentration of EAK16-I with that of EAK16-II

It is useful to compare the critical self-assembly concentration of EAK16-I with that of a similar ionic-complementary peptide, EAK16-II (AEAEAKAKAEAEAKAK). Fung *et al*. [13] studied the concentration dependence of the self-assembly of EAK16-II and found that the critical aggregation concentration of EAK16-II was around 0.1 mg/ml, whereas in the present study for EAK16-I it was found to be 0.3 mg/ml. EAK16-I and II have the same amino acid composition, Ala, Glu, and Lys, but a different charge distribution ($-+-+-+-+$ for EAK16-I vs. $--++--++$ for EAK16-II) and thus polarity. This seems to indicate that a slight decrease in the polarity of the peptide caused an increase in the critical self-assembly concentration.

Fung *et al*. also observed that there was a small "dip" in the plot of surface tension with peptide concentration for EAK16-II [13]. The small dip in the surface tension plot has been known to occur in the presence of hydrophobic impurities [31]. However, this small dip was not observed for EAK16-I, although the EAK16-I sample was expected to have impurities similar to those of EAK16-II. The absence of the "dip" in the surface tension plot of EAK16-I may thus indicate that the self-assemblies of EAK16-I are more surface active than the impurities. In fact, the surface tension value of EAK16-I at plateau (*ca*. 57 mJ/m^2) was lower than that of EAK16-II (*ca*. 60 mJ/m^2) and also slightly lower than the minimum in the surface tension dip of EAK16-II (*ca*. 58 mJ/m^2; see Figure 3 in Fung *et al.* [13]), supporting the hypothesis.

Critical Self-assembly Concentration Determined by Nanostructure Observations

In conjunction with the surface tension measurements, AFM images were acquired to characterize the self-assembled nanostructures. AFM images of the EAK16-I nanostructures at various concentrations are shown in Figure 4. Two structural transitions were observed. The first structural transition occurred at 0.05 mg/ml, where a transition from globular (0.01 and 0.025 mg/ml) to fibrillar structures (above 0.05 mg/ml) was observed. Above this concentration, no globular structures were observed, and therefore the transition from globular to fibrillar structures appears to be 100%. This transition was not observed in the surface tension data. The size of these fibrillar assemblies was roughly constant over the concentration range (0.05 to 0.2 mg/ml). The second structural transition occurred at the peptide concentrations of 0.3 mg/ml, which corresponded with the abrupt change in the surface tension (Figure 3). At this point, the fibrillar structures underwent a transition to thicker fibers. To ensure that the nanostructural transition observed is not induced by the substrate, we used graphite (a hydrophobic surface), in addition to mica, as the sample support during the AFM imaging. We found the fibrillar structures on both graphite and mica surfaces.

The change in fibril morphology is reflected in the quantitative analysis of the AFM images. Various size parameters were plotted as a function of EAK16-I concentration (Figure 5). The average width, height, and equivalent radius of the fibrillar assemblies that were observed above a peptide concentration of 0.05 mg/ml were plotted as a function of peptide concentration. The width observed by AFM was corrected for the finite tip size of the AFM probe, following a procedure described by Fung *et al*. [13]. The equivalent radius calculation was based on the assumption that the assemblies had a circular cross section, although the nanostructures observed were more like twisted ribbons (large widths compared with small heights in Figure 5). The resulting radii were plotted as a function of the peptide concentration (Figure 5c). The average widths of fibrils formed over the concentrations between 0.05 and 0.2 mg/ml were similar. When the concentration reached 0.3 mg/ml, however, the average width started to increase and reached a plateau value, although with some variations. The average height also showed a slight increase at concentrations greater than 0.3 mg/ml (Figure 5b). Figure 5c shows that there is a transition point in the equivalent radius at concentrations around 0.3 mg/ml. The equivalent radii of fibrils that were formed between 0.05 and 0.2 mg/ml are around 10 nm, whereas the equivalent radii

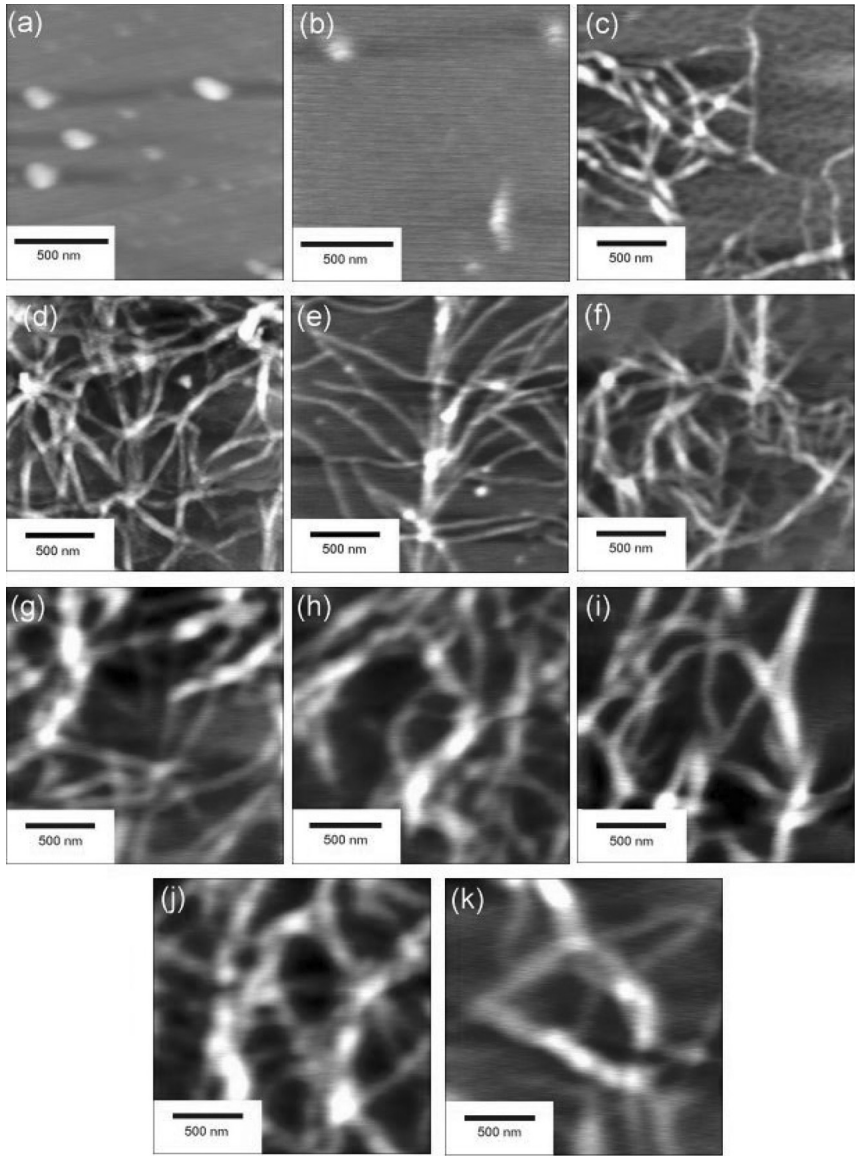

FIGURE 4 AFM images of EAK16-I assemblies at various peptide concentrations: (a) 0.01, (b) 0.025, (c) 0.05, (d) 0.075, (e) 0.1, (f) 0.2, (g) 0.3, (h) 0.5, (i) 0.8, (j) 1.0, and (k) 2.0 mg/ml . See Figure 5 for detailed dimensional analysis.

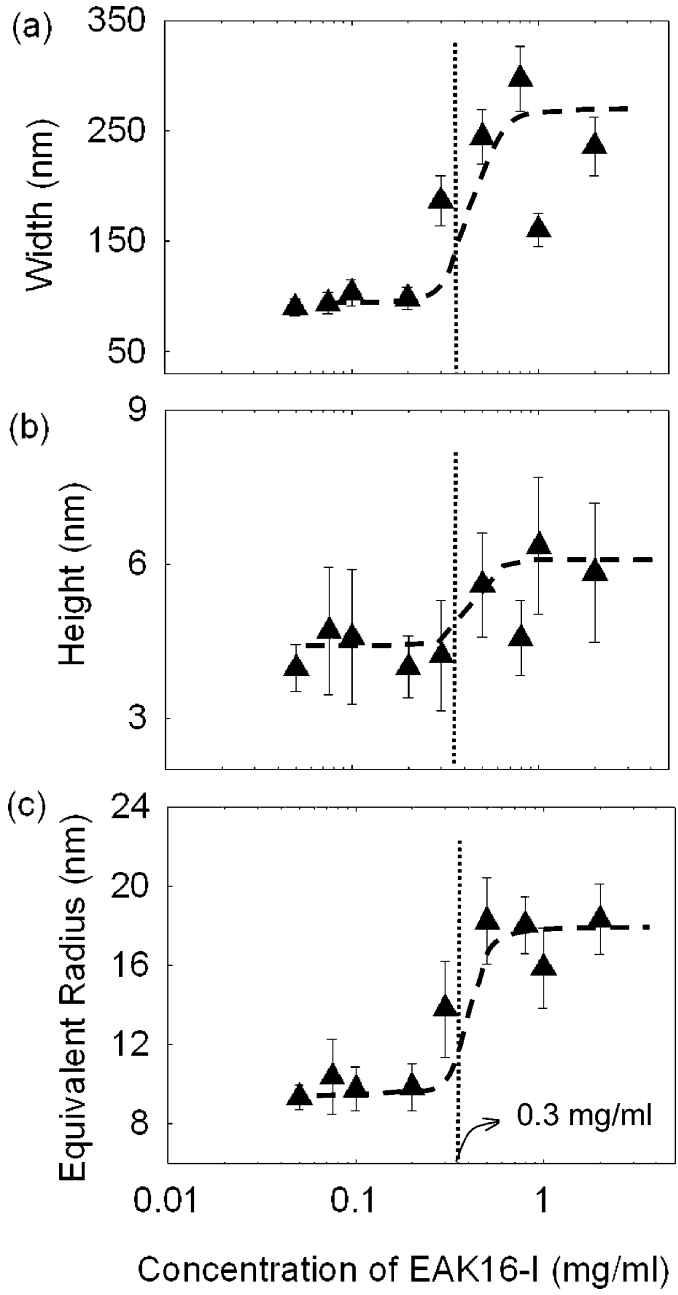

FIGURE 5 Average dimensions of EAK16-I assemblies: (a) average width, (b) average height, and (c) equivalent radius. The equivalent radius was determined based on an assumption of a circular cross section for the fiber (see text).

of fibers that formed above concentrations of 0.3 mg/ml are close to 20 nm, which is approximately double the size of those of fibrils observed at concentrations below 0.3 mg/ml.

Comparison of Structural Transitions of EAK16-I with EAK16-II

The presence of two structural transitions of EAK16-I is of interest. Fung *et al*. [13] observed one structural transition in their AFM study of EAK16-II, which occurred at a peptide concentration of *ca*. 0.1 mg/ml, below which globular assemblies coexisted with short filaments and above which globular assemblies disappeared and fibrillar structures formed (see Figure 7 in Fung *et al*. [13]). Their observation resembles the first structural transition of EAK16-I, from globular assemblies to fibrillar ones at a concentration of 0.05 mg/ml (Figure 4). The size of fibrils formed by both EAK16-I and II are comparable. The width of the EAK16-II fibrils was found to be around 50–70 nm [13], whereas the width of EAK16-I fibrils was around 80–90 nm (Figure 5a). The EAK 16-I fibril formation at a lower concentration seems to be related to the charge distribution of the peptide. Recently, Jun *et al*. [14] studied the single molecular properties of EAK16-I, II and IV using Monte Carlo simulations; they showed that the least-polar EAK16-I had the largest tendency to form stretched structures, which facilitate fibrillogenesis. This tendency of EAK16-I may explain why fibrils formed at a lower concentration for EAK 16-I than for EAK16-II.

The second structural transition from fibrils to fibers appears unique for EAK16-I. The surface tension of EAK 16-I solution reached a constant plateau value only at concentrations above 0.3 mg/ml (Figure 4), where the second structural transition from fibrils to fibers occurred. The first structural transition from globular assemblies to fibrils was not reflected in Figure 4. This is probably because the self-assembled monolayers of peptide fibrils do not "saturate" the air–water interface. Fibers of larger size compared with fibrils appear to be more effective in saturating the interface, resulting in a surface tension plateau. It should be emphasized that although the differences in surface tension and nanostructure between the two peptides are attributed to their different charge distributions, the exact molecular mechanisms underlying these differences are still unknown.

The structural transitions involved in the self-assembly of EAK16-I resemble those from protofibrils to fibrils observed with numerous naturally occurring peptides. Thus, an understanding of this structural transition has implications in the analysis and treatment of peptide/protein conformational diseases; in addition, it can be applied to the construction of self-assembled peptide/protein nanostructures.

Effect of NaCl on the Self-assembly of EAK16-I

NaCl is known to decrease the CMC of typical ionic surfactants by charge screening of the ionic headgroups [32, 33]. The estimated equilibrium surface tension and induction time, as a function of EAK 16-I concentration, are plotted in Figures 6a and 6b, respectively. The peptide critical self-assembly concentration in the presence of 20 mM NaCl was 0.8 mg/ml, above which the surface tension and the induction time reached a plateau. The surface tension value at the plateau was *ca*. 55 mJ/m^2 in the presence of NaCl, compared with *ca*. 57 mJ/m^2 without NaCl, indicating that the assemblies of EAK16-I that formed in the presence of NaCl are slightly more surface active than those formed without NaCl. This decrease in surface tension may be explained by the fact that NaCl can screen the charge interaction of the EAK16-I molecules or self-assemblies, making them less hydrophilic or more hydrophobic overall.

The increase in the "critical self-assembly concentration" by adding 20 mM NaCl was surprising, as the addition of salts has been shown to facilitate the self-assembly of peptides [15–17] and decrease the CMC of surfactants [32, 33]. It is also noted that the "critical self-assembly concentration" reflected by surface tension measurements corresponds to the second structural transition from fibrils to fibers. The spectrum of EAK 16-I nanostructures in the presence of NaCl is shown in Figure 7. At the lowest peptide concentration used (0.01 mg/ml), EAK16-I formed fibrils that were different from the globular structures that formed without NaCl at the same peptide concentration. This observation indicates that the presence of NaCl facilitates fibril formation, as has been shown in other studies [15–17]. The fibrils were observed over a peptide concentration range from 0.01 to 0.6 mg/ml. At 0.8 mg/ml, fibrillar assemblies of EAK16-I underwent a structural transition to larger fibers. Quantitative analysis of the AFM images is given in Figure 8. Relatively small assemblies of EAK16-I were formed in the presence of NaCl. The average width of the fibrils was around 30–40 nm, and the average width of the fibers was around 100–120 nm (Figure 8a), which are smaller in comparison with 80–90 and 200–250 nm, respectively, in the absence of NaCl (Figure 5a). The average heights of fibrils and fibers did not change significantly in response to peptide concentration changes and were around 1.5–2 nm, corresponding to 2–3 layers of β-sheets (Figure 8b). The equivalent radius calculated from the cross-sectional area, with an assumption of a circular cross section, is given in Figure 8c. There is an abrupt increase in the equivalent radius from 5 to 10 nm at a concentration of 0.8 mg/ml.

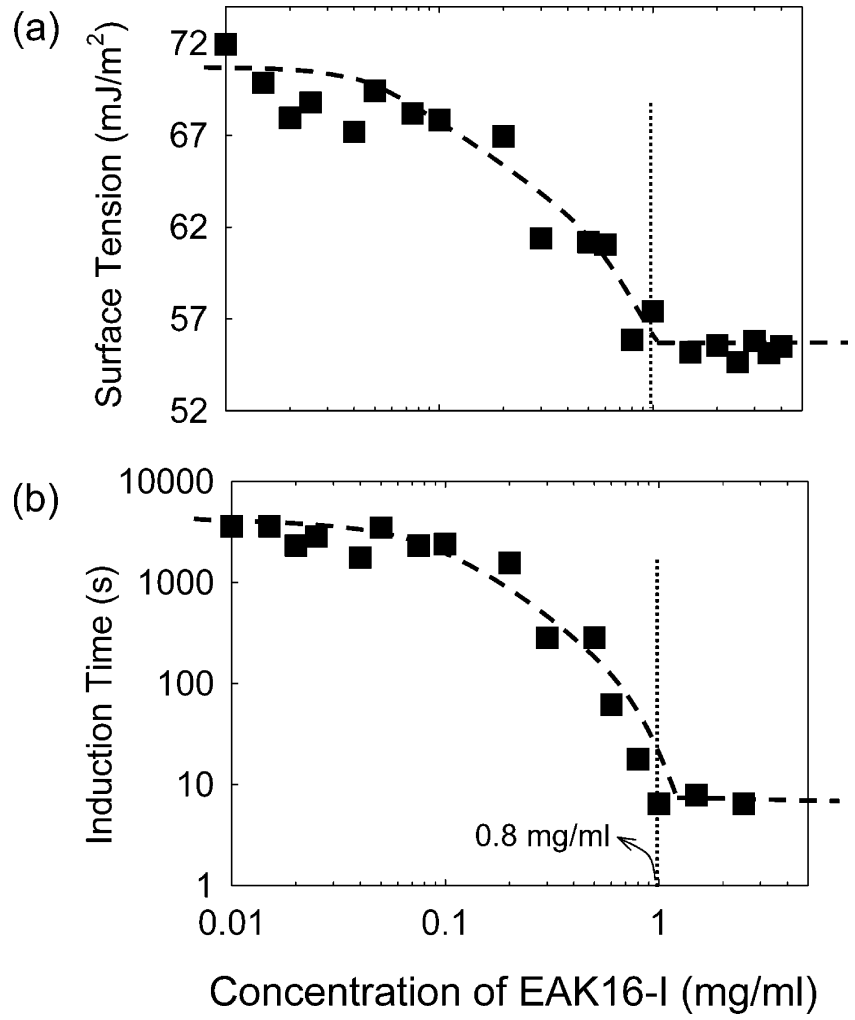

FIGURE 6 (a) Estimated surface tension and (b) the induction time for various concentrations of EAK16-I in the presence of 20 mM NaCl. The equilibrium surface tension was determined by the "end points" method (see text), and the induction time was determined as the time when the surface tension was decreased 5% from the initial value.

This abrupt increase in the equivalent radius correlates with the structural transition from fibrils to fibers.

To confirm further the effect of NaCl on the fibril formation, various concentrations of NaCl were added to an EAK16-I solution at a

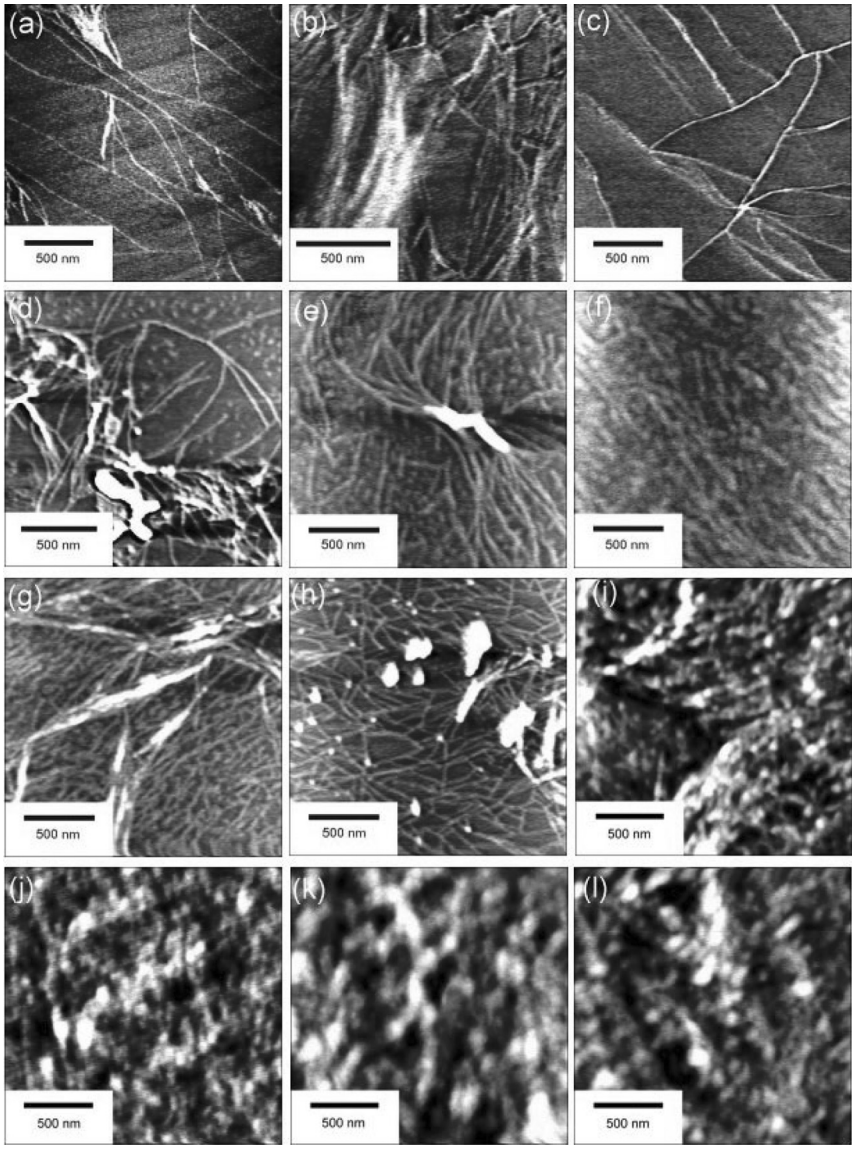

FIGURE 7 AFM images of EAK16-I assemblies in the presence of 20 mM NaCl at various peptide concentrations: (a) 0.01, (b) 0.025, (c) 0.05, (d) 0.075, (e) 0.1, (f) 0.2, (g) 0.3, (h) 0.6, (i) 0.8, (j) 1.0, (k) 2.0, and (l) 3.0 mg/ml.

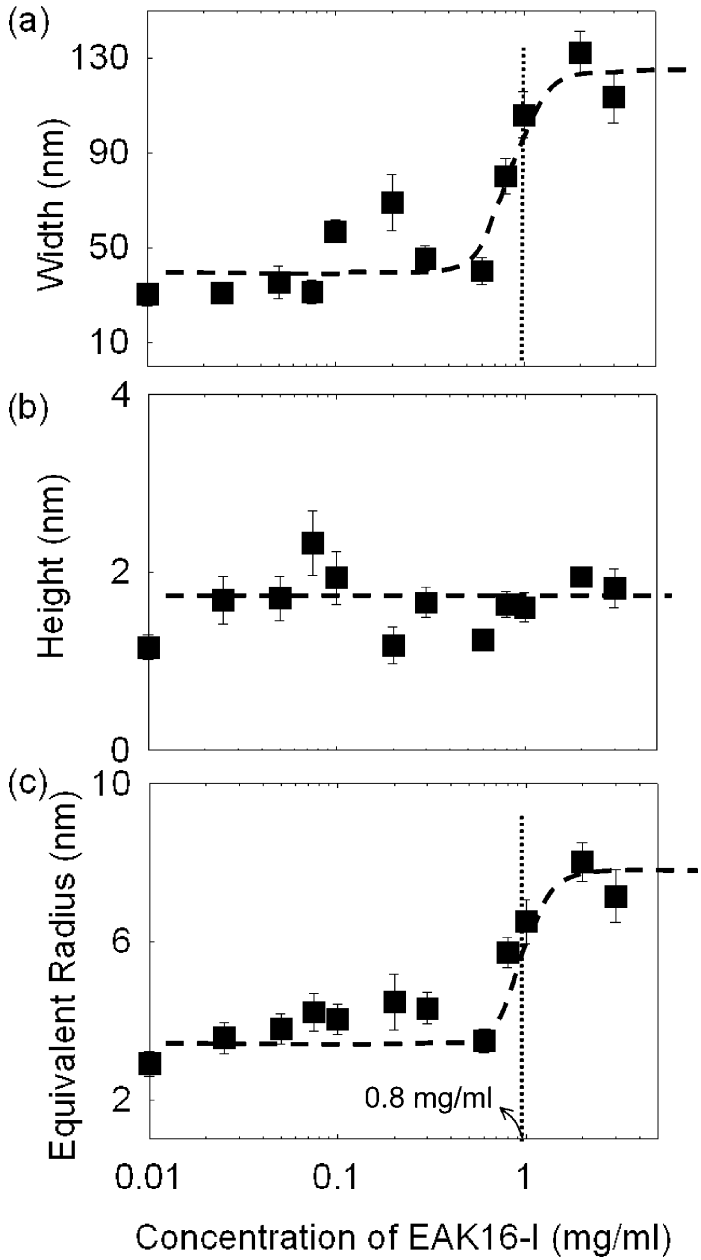

FIGURE 8 Average dimensions of EAK16-I assemblies in the presence of 20 mM NaCl: (a) average width, (b) average height, and (c) equivalent radius. The equivalent radius was determined based on an assumption of a circular cross section for the fiber (see text).

concentration of 0.01 mg/ml. The nanostructures of each solution were investigated with AFM (Figure 9). At 0.1 mM NaCl, EAK16-I only formed globular structures (Figure 9a). In the presence of 5 mM NaCl, short, thin fibrillar fragments of EAK16-I formed (Figure 9b), and long fibrillar assemblies were observed at 10 or 20 mM NaCl (Figures 9c and 9d). NaCl facilitates the fibril formation, which has also been observed for other peptide self-assemblies [15, 16, 34].

It is well known that ionic salts influence the stability and conformation of various macromolecules by charge screening. EAK16-I has a hydrophilic face with eight ionic side groups. When NaCl is added, the charges of the ionic side of the EAK16-I are screened, and the peptide molecule becomes less hydrophilic, allowing the peptide to self-assemble into fibrils at lower concentrations. In the presence of

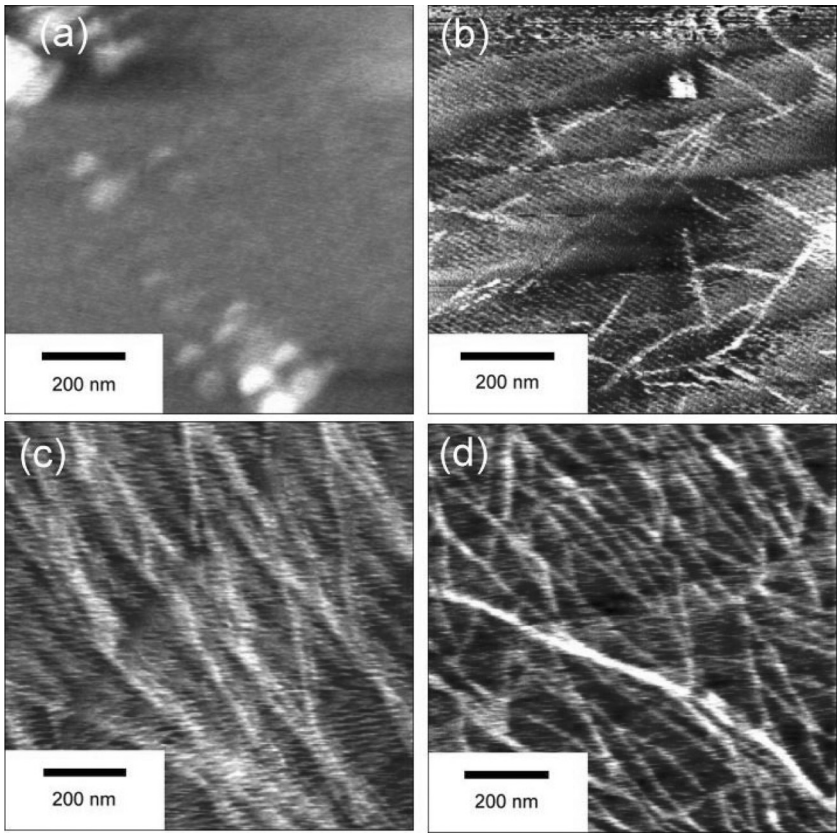

FIGURE 9 The AFM images of EAK16-I at 0.01 mg/ml at various concentrations of NaCl: (a) 0.1, (b) 5, (c) 10 and (d) 20 mM.

NaCl the second structural transition from fibrils to fibers occurred at a higher concentration, compared to that without NaCl. This may support the argument that the intermolecular forces governing the formations of fibrils and fibers are different: the fibril formation is related to the hydrophobic interaction, and the fiber formation is more related to the electrostatic interaction. Without NaCl, the fibrils can stack together by electrostatic interactions between each other to form larger fibers. In the presence of NaCl, however, the charges of EAK16-I are screened by NaCl, weakening the electrostatic interaction between fibrils. Consequently, the fibers can form only at a higher concentration in the presence of NaCl.

CONCLUSIONS

The concentration dependence of peptide self-assembly of an ionic-complementary peptide, EAK16-I, was investigated using surface tension measurements and nanostructure observations. The former revealed that the surface tension decreases with increasing peptide concentration and that there is a critical self-assembly concentration, 0.3 mg/ml, above which the surface tension is unaffected by further increasing peptide concentration. The morphology of the self-assembled nanostructure as observed by AFM showed two structural transitions. The first structural transition occurred at 0.05 mg/ml, where globular nanostructures underwent a transition to fibrils, and this transition was not reflected in the surface tension measurements. The second structural transition occurred at 0.3 mg/ml, where the fibrils changed to thicker fibers, which corresponded to the critical self-assembly concentration as determined by the surface tension measurements. These structural transitions of EAK16-I are different from that of EAK16-II. The differences between EAK 16-I and II in self-assembly were attributed to their different charge distributions. The effect of ionic salt NaCl on the peptide self-assembly was also investigated using the same techniques. The addition of NaCl decreased the first critical concentration ($0.05 \rightarrow 0.01$ mg/ml) where the morphological transition from globules to fibrils occurred. The addition of NaCl increased the second critical self-assembly concentration ($0.3 \rightarrow 0.8$ mg/ml), where the structural transition from fibrils to fibers occurred.

REFERENCES

[1] Holmes, T. C., de Lacalle, S., Su, X., Liu, G., Rich, A., and Zhang, S., *Proc. Natl. Acad. Sci. USA* **97**, 6728–6733 (2000).

[2] Nowak, A. P., Breedveld, V., Pakstis, L., Ozbas, B., Pine, D. J., Pochan, D., and Deming, T. J., *Nature* **417**, 424–428 (2002).

[3] Zhang, S., Marini, D. M., Hwang, W., and Santoso, S., *Curr. Opin. Chem. Biol.* **6**, 865–871 (2002).
[4] Hartgerink, J. D., Beniash, E., and Stupp, S. I., *Science* **294**, 1684–1688 (2001).
[5] Vauthey, S., Santoso, S., Gong, H., Watson, N., and Zhang, S., *Proc. Natl. Acad. Sci. USA* **99**, 5355–5360 (2002).
[6] Whaley, S. R., English, D. S., Hu, E. L., Barbara, P. F., and Belcher, A. M., *Nature* **405**, 665–668 (2000).
[7] Zhang, S., *Biotech. Adv.* **20**, 321–339 (2002).
[8] Knichel, M., Heiduschka, P., Beck, W., Jung, G., and Gopel, W., *Sensors Actuators B* **28**, 85–94 (1995).
[9] Lowe, C. R., *Curr. Opin. Struct. Biol.* **10**, 428–434 (2000).
[10] Strong, A. E. and Moore, B. D., *Chem. Commun.* **4**, 473–474 (1998).
[11] Strong, A. E. and Moore, B. D., *J. Mater. Chem.* **9**, 1097–1105 (1999).
[12] Hong, Y., Legge, R. L., Zhang, S., and Chen, P., *Biomacromolecules* **4**, 1433–1442 (2003).
[13] Fung, S. Y., Keyes, C., Duhamel, J., and Chen, P., *Biophys. J.* **85**, 537–548 (2003).
[14] Jun, S., Hong, Y., Imamura, H., Ha, B. Y., Bechhoefer, J., and Chen, P., *Biophys. J.* **87**, 1249–1259 (2004).
[15] Zhang, S., Holmes, T., Lockshin, C., and Rich, A., *Proc. Natl. Acad. Sci. USA* **90**, 3334–3338 (1993).
[16] Zhang, S., Lockshin, C., Cook, R., and Rich, A., *Biopolymers* **34**, 663–672 (1994).
[17] Caplan, M. R., Moore, P. N., Zhang, S., Kamm, R. D., and Lauffenburger, D. A., *Biomacromolecules* **1**, 627–631 (2000).
[18] Brack, A. and Orgel, L. E., *Nature* **256**, 383–387 (1975).
[19] Nandi, P. K. and Robinson, D. R., *J. Am. Chem. Soc.* **94**, 1299–1308 (1972).
[20] Piculell, L. and Nilsson, S., *Prog. Colloid Polym. Sci.* **82**, 198–210 (1990).
[21] Tu, E. B., Ji, G. Z., and Jiang, X. K., *Langmuir* **13**, 4234–4238 (1997).
[22] Borisov, O. V. and Zhulina, E. B., *Macromolecules* **35**, 4472–4480 (2002).
[23] Zhang, L., Somasundaran, P., and Maltesh, C., *Langmuir* **12**, 2371–2373 (1996).
[24] Dutkiewicz, E. and Jakubowska, A., *Colloid Polym. Sci.* **280**, 1009–1014 (2002).
[25] Ropers, M. H., Czichocki, G., and Brezesinski, G., *J. Phys. Chem. B*, **107**, 5281–5288 (2003).
[26] Khan, M. O., Melnikov, S. M., and Jonsson, B., *Macromolecules*, **32**, 8836–8840 (1999).
[27] Korolev, N. and Nordenskiold, L., *Biomacromolecules* **1**, 648–655 (2000).
[28] Chen, P., Lahooti, S., Policova, Z., Cabrerizo-Vilchez, M. A., and Neumann, A. W., *Colloids Surf. B: Biointerfaces* **6**, 279–289 (1996).
[29] Miller, R., Aksenenko, E. V., Fainerman, V. B., and Pison, U., *Colloids Surf. A: Physicochem. Eng. Aspects* **183**, 381–390 (2001).
[30] van der Vegt, W., Norde, W., van der Mei, H. C., and Busscher, H. J., *J. Colloid Interface Sci.*, **179**, 57–65 (1996).
[31] Clint, J. H., *Surfactant Aggregation* (Blackie & Son Ltd., New York, 1992).
[32] Miyahishi, S., Okada, K., and Asakawa, T., *J. Colloid Interface Sci.* **179**, 57–65 (2001).
[33] Hiemenz, P. C. and Rajagopalan, R., *Principles of Colloid and Surface Chemistry* (Marcel Dekker, Inc., New York, 1997), pp. 355–404.
[34] López de la Paz, M., Goldie, K., Zurdo, J., Lacroix, E., and Dobson, C. M., *Proc. Natl. Acad. Sci. USA* **99**, 16052–16057 (2002).